A magnetorheological fluid damper for rotor applications

Paola Forte, Marco Paternò, Emiliano Rustighi

Dipartimento di Ingegneria Meccanica, Nucleare e della Produzione, Università di Pisa, Pisa, Italy

In the last decade there has been an increasing attention toward the employment of electrorheological (ER) and magnetorheological (MR) fluids in active bearings and active squeeze film dampers in rotordynamics even though we are still far from industrial applications. MR fluids react to magnetic fields undergoing changes in their mechanical characteristics, viscosity and stiffness in particular. In the literature some applications of ER fluids in rotor squeeze film dampers can be found. On the contrary little is reported on similar test rigs set up for MR dampers. In this work the design of a MR squeeze film damper is presented and discussed. A numerical simulation has been carried out in order to evaluate the dynamic behaviour of the damped rotor as function of the magnetic field strength. The test rig is made of a slender shaft supported by two oilite bearings and an unbalanced disk. The damper is interfaced with the shaft through a rolling bearing. Electric coils generate the magnetic field whose field lines cross the MR film. Since the damping characteristics can be varied continuously by controlling the magnetic field, it is possible to have the optimum conditions for each regime of rotational speed. Preliminary tests are encouraging.

Keywords: active damper, rotordynamics, magnetorheological fluid, critical speed, test rig.

1. Introduction

The problem of vibrations in rotordynamics is commonly faced with passive squeeze fluid film or elastomeric dampers. Unfortunately their effect varies with the rotor speed; experimental evidence shows that in order to dissipate energy at the critical speeds the rotor displacement in the damper has to be significant, meaning that viscosity must be low. On the contrary in non critical conditions higher values are required [1]. In the last decade there has been an increasing attention toward the employment of electro-rheological (ER) and magneto-rheological (MR) fluids, suspensions of micron-sized dielectric/ferromagnetic particles respectively which, when subjected to electric/magnetic fields, undergo changes in their mechanical characteristics, viscosity and stiffness in particular. Their macroscopic behaviour is represented by the Bingham plastic model. These "smart" materials have been successfully used in valves, dampers and clutches and adaptive structures [2-5] but we are still far from industrial applications in rotordynamics.

In the literature theoretical and experimental studies on the employment of ER fluids in active journal bearings and squeeze dampers [6-11] are reported. More limited information is available to date regarding MR fluids. In fact while general aspects and applications of MR fluids have been dealt with to some extent [12-15] showing their promising characteristics, only quite recently some paper has appeared on rotor dampers [16].

In this work the theoretical modeling, the design and the preliminary testing of a MR squeeze film damper are presented and discussed.

2. Nomenclature

R, R_o, R_i	journal radius, inner and outer radii	ε	eccentricity ratio (e/c)
h	film thickness	p, p^*	pressure
x	spatial coordinate, sliding direction	q	volume flow rate/axial length
y, y^*	spatial coordinate, direction across film	e	bearing eccentricity
z	spatial coordinate, normal to x,y	μ	fluid viscosity
θ	angular coordinate (x/R)	μ_0	vacuum magnetic permeability
u, u^*, v, w	fluid velocity in x,y,z directions	μ_r	relative magnetic permeability
c	bearing radial clearance	τ_0, τ_0^*	yield shear stress
l	shaft length	ω	precession speed
a	distance damper – shaft end	L	bearing axial length
k_{11}, k_{12}, k_{22}	shaft stiffness coefficients	X_1, Y_1	coordinate system (disk location)
kg	squirrel cage stiffness coefficient	X_2, Y_2	coordinate system (damper location)
md	disk mass		

mg	grain mass
M_1	unbalanced disk mass (md+mg)
M_2	journal mass

δ	unbalance distance of mass center
β	mass center rotation with respect to X_1
B_{MR}	magnetic field in the MR fluid
J_S	current density in the coils

$(\ )^*$	dimensionless quantity

3. Modeling of the Magnetorheological fluid.

In this paper we follow the analysis performed by Tichy [7] for the lubrication of the one- dimensional bearing illustrated in Fig.1 where $u >> v$, $\partial/\partial x >> \partial/\partial y$, and $w = \partial/\partial z = 0$.

In this case, one obtains for the so called Bingham model:

$$\frac{\partial u}{\partial y} = 0 \qquad \text{for } |\tau| \le |\tau_0|\ ; \qquad \tau = \tau_{xy} = \mu \frac{\partial u}{\partial y} \pm \tau_0 \qquad \text{for } |\tau| > \tau_0 \qquad (1)$$

meaning that for shear stress magnitude $|\tau|$ greater than a yield shear parameter τ_0, the material flows as a Newtonian fluid with viscosity μ; otherwise the material remains rigid. For the squeeze film damper, the film thickness is defined as:

$$h = c(1 + \varepsilon \cos \theta) \qquad (2)$$

Fig.1. Schematic of damper geometry

where c is the bearing radial clearance, $c = R_0 - R_i << R_0 \approx R$, ε is the eccentricity ratio, $\varepsilon=e/c$, θ is the angular coordinate measured from the maximum film thickness location and $x=R\theta$. Therefore, the selected coordinate system rotates with the journal at a constant speed ω. For any non-zero τ_0 the implicit form of the Reynolds equation is obtained:

$$\left(h\frac{dp}{dx}\right)^3 + 3\left(\frac{dp}{dx}\right)^2\left[4\mu(\omega Rh + q) \pm h^2\tau_0\right] - (\pm 4\tau_0)^3 = 0 \qquad (3)$$

The $+\tau_0$ condition is used when dp/dx is negative and vice versa. Eqn. (3), being a cubic equation, has a standard analytical solution for dp/dx. However, any of the three roots may be the physically meaningful one, depending on the value of the parameters. The pressure is determined by integrating the pressure gradient expression and adjusting the constant flow rate q so as to satisfy the periodicity condition $p(0,q)=p(2\pi,q)$:

$$p(\theta,q) = \int_0^\theta \frac{dp}{d\theta}d\theta + p(0,q). \qquad (4)$$

Figure 2 shows typical dimensionless velocity profiles ($u^*=u/U$, $y^*=y/h$) for various values of the dimensionless yield shear stress parameter $\tau^*_0=\tau_0 c/(\mu U)$. The surfaces are both sliding in the reverse direction with $U_1=U_2=-U$. The flow is symmetric about the midplane $y=h/2$, where the shear stress is zero. In the Newtonian case, a Poiseuille flow takes place with a uniform negative velocity superimposed. It is observed that as the yield stress τ_0 increases, a floating core thickens about the midplane.
The core thickens with increasing τ_0^* and fills the gap at two locations where $h/c=q^*$. The radial and tangential forces on the rotor due to the film pressure (see fig.1) are found by performing the following integrations:
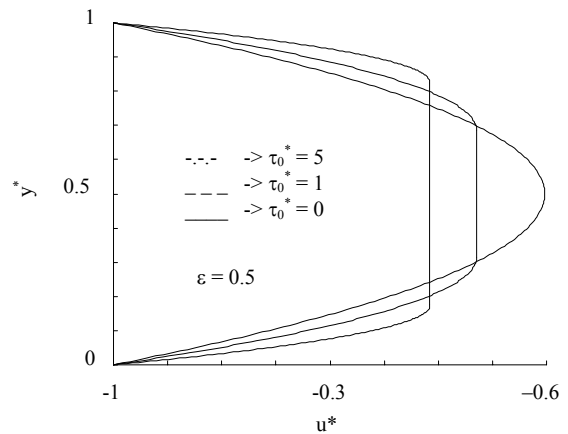
Fig.2. Typical velocity profiles

$$F_r = RL \int_{\pi}^{2\pi} p\cos\theta d\theta \qquad F_t = RL \int_{\pi}^{2\pi} p\,\text{sen}\,\theta d\theta \qquad\qquad (5)$$

in which simple cavitation conditions are assumed (π film). In order to obtain some data to design the actualdamper the dimensional form is preferable and the values reported in the following table were assumed.

Table.1:
Numerical values used in damper calculation.

L	c	R	μ
2 cm	2.5 mm	3.2 cm	0.18 Pa*s

The fluid used is the oil based MR fluid MRF 132 – LD produced by the Lord Corporation. An average value for the viscosity was considered neglecting the so called "shear thinning effect", i.e, the relationship between viscosity and shear rate.

Radial and tangential forces were calculated considering different values for the yield stress (τ_0 = 500, 10000, 20000 Pa) and for the whirling velocity (ω = 50, 500, 1000 rad/sec).

Tangential Force:

ω=50 rad/sec $\qquad\qquad$ ω=500 rad/sec $\qquad\qquad$ ω=1000 rad/sec

Radial Force

ω=50 rad/sec $\qquad\qquad$ ω=500 rad/sec $\qquad\qquad$ ω=1000 rad/sec
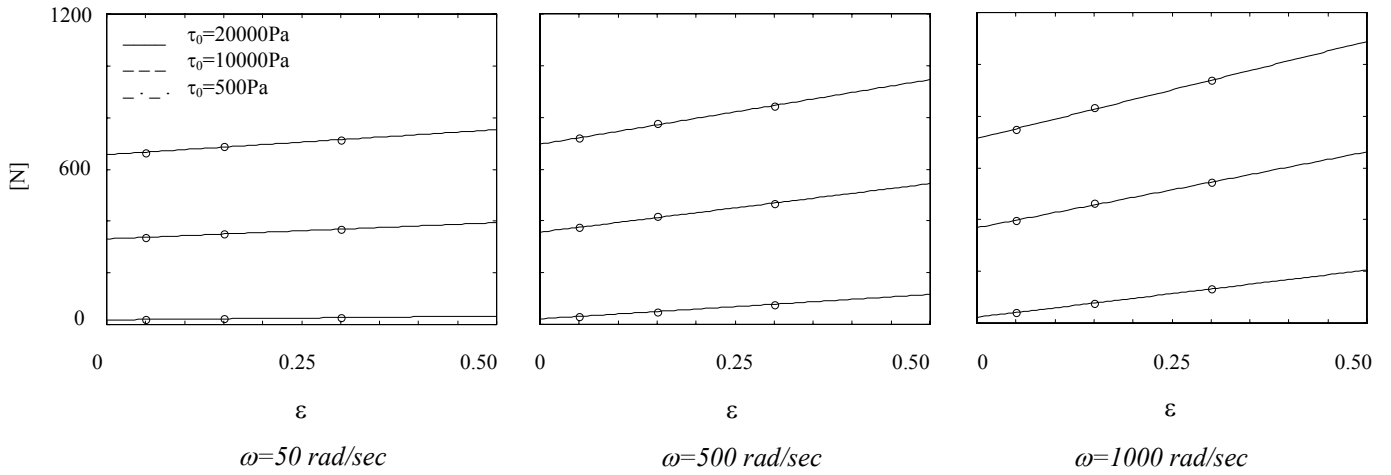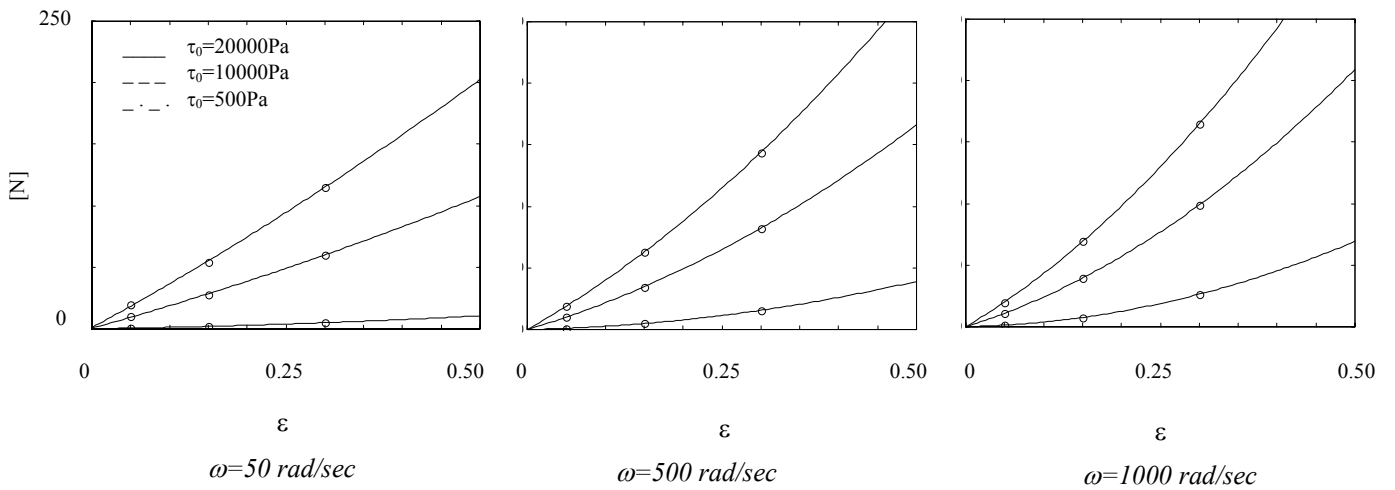
Fig.3. Radial and tangential forces due to the pressure field in the gap

Both the radial and tangential forces increase with the yield shear stress. Thus the tangential force has a finite value when $\varepsilon \to 0$. Such behaviour can be explained considering Bingham's fluid constitutive equation.

Figure 3 suggests the following analytical expressions for F_t and F_r:

$$F_t = \left[a_t(\omega, \tau_0) + b_t(\omega, \tau_0) \cdot \left(\frac{e}{c} \right) \right]; \qquad\qquad F_r = \left[a_r(\omega, \tau_0) \cdot \left(\frac{e}{c} \right)^2 \right] \qquad\qquad (6)$$

4. Modeling of the rotor – damper system
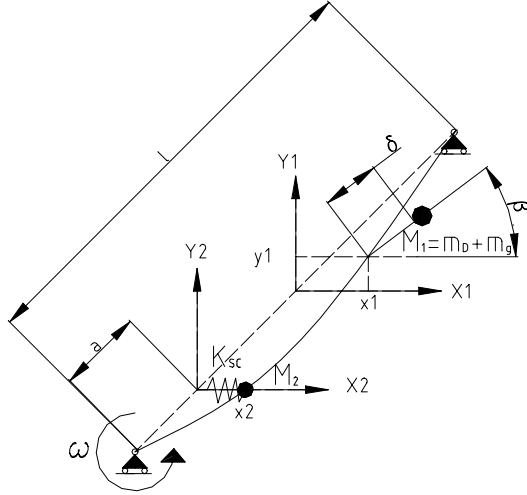
Fig.4. Schematic model of the rotor – damper system

In figure 4 the schematic model of the rotor-damper system is presented. It is made of an elastic shaft, with a disk with mass m_D connected in the middle, hinged at both ends.

The shaft is also supported by the squeeze-film damper. Two coordinate systems rotating with the shaft at its whirling velocity ω are defined. The center of mass of the disk is offset by a distance δ from the geometric center of the shaft due to the unbalance, m_g. Thus, the unbalance vector makes a constant arbitrary angle β with respect to the X_1 direction. The coordinates (x_1, y_1) describe the displacement of the geometric center of the disk while x_2 describes the radial displacement of the inner cylinder of the damper (see Par. 5 for the description of the device). The damper is accounted for by adding a second mass, M_2, to the shaft.

The tangential force due to the pressure generated in the damper acts in the Y_2 direction while the radial force acts in the X_2 direction. The inner cylinder of the damper is constrained by a "squirrel cage" (see par. 5.1) which is accounted for in the analytical model by adding a radial stiffness, K_{sc}. The four unknown values x_1, y_1, x_2 and β can be found by writing and solving the four equilibrium equations written in the X_1, X_2, Y_1 and Y_2 directions. In these equations we consider the centrifugal forces due to the masses M_1 and M_2, the elastic reactions of the shaft (using the linearized stiffness coefficient k_{11}, k_{12}, k_{22}), and the possible damper reaction:

$$\begin{cases} k_{11}x_1 + k_{12}x_2 = M_1\omega^2(x_1 + \delta \cos \beta) \\ k_{11}y_1 = M_1\omega^2(y_1 + \delta \sin \beta) \\ k_{12}x_1 + k_{22}x_2 + k_{sc}x_2 + F_r(\omega, \tau_0) = M_2\omega^2 x_2 \\ k_{12}y_1 + F_t(\omega, \tau_0) = 0 \end{cases} \qquad\qquad (7)$$

Equations (7) are solved for several values of the yield stress and for angular velocities varying from *0* up to *10000 rpm*. That is actually the range of velocities which can be explored using the *Bently Nevada Rotor Kit* (see Par. 6).

For every ω and τ_0 four solutions are found among which the physically meaningful one is chosen. When no meaningful solution arises it means that the forces due to unbalance aren't high enough to break the columnar structures created in the MR fluid and the damper acts on the shaft as a rigid constraint.

The numerical values used in the simulation are reported in the following table.

Table 2:
Numerical values for the simulation of the damped operation.

l	a	k_{11}	k_{12}	k_{22}	k_{sc}	m_d	m_g	M_1	δ	M_2
42 cm	11 cm	452140 N/m	-539820 N/m	756200 N/m	174000 N/m	0.800 Kg	7 g	0.807 Kg	2.625*10⁻⁴ m	0.400 Kg

In figure 5 the radial displacement of the geometric centre of the disk placed in the middle of the shaft versus the angular velocity of the shaft is shown:
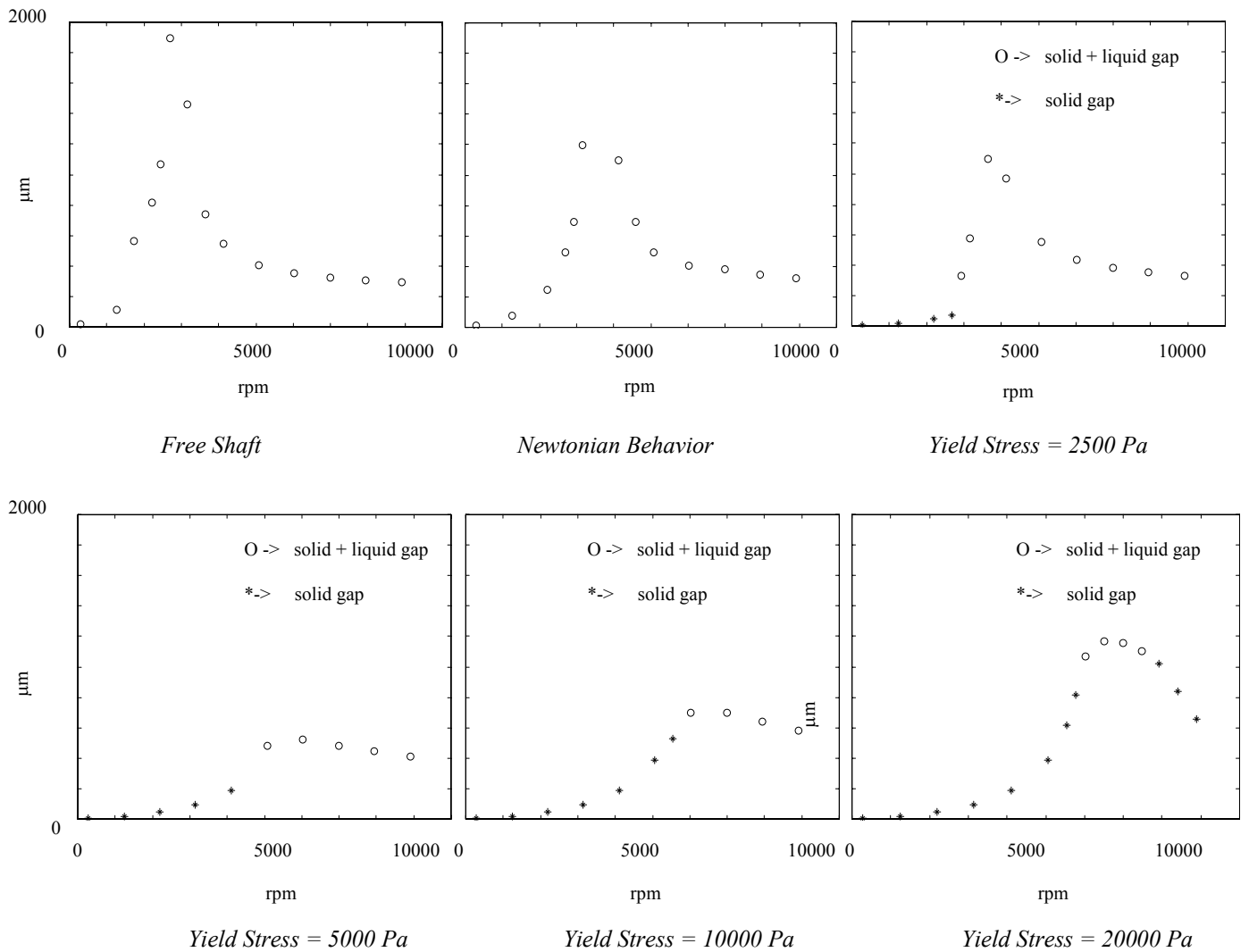
Fig.5. Effects of the fluid yield stress increase on the rotor behaviour

The results shown above suggest two different ways to control the shaft dynamic instability:

o the first is a simple on – off procedure consisting in turning the device on while the shaft is passing through the critical speed and turning it off when the displacements start to increase again; when the device is active, the magnetic field applied on the fluid has to be high enough to maintain the fluid solid in every zone of the gap.

o the second procedure consists in setting the magnetic field at a constant value to obtain the shaft behaviour shown in figure 5 (yield stress = 5000 Pa).

The limit of this calculation is that it doesn't consider the effects of the magnetic field on the mobile parts of the damper but the solution of this complex problem is beyond the scope of this work.

5 Design of the MR damper

5.1 Description of the device

Figure 6 presents the longitudinal section of the device. It is entirely made of C40 steel except for the squirrel cage and the the shaft bush made of an aluminium alloy. Each coil has 240 windings of a $\phi=0.63mm$ wire capable of bearing a constant current of *1A,* value that can rise up to *2A* for a limited time. The wires coming out of the coils are connected to each other so that the two coils are run by the current in opposite directions.

The rotation of the transversal section of the deformed shaft *(ϕ = 10mm)* is allowed by an orientable radial bearing. The basic parameters of the MR film are the same shown in table 1.

The radial clearance was set at a dimension *c =2.5mm* after noticing that a smaller gap would have produced a damping effect with too low values of the yield stress not taking advantage of the potential characteristics of the MR fluid. Moreover

due to the small dimensions of the *Bently Nevada Rotor Kit* used to test our device, it's impossible to create centrifugal forces high enough to be balanced by the pressure generated in a gap smaller than *2.5mm*. Finally, with a too small gap, there is a higher risk of lock up of the damper due to the magnetic pull force between its moving parts.

Since one of the aims of the work is to verify the theoretical model the damper is devised with one single gap and as long as possible in order to satisfy the one – dimensional bearing hypothesis and neglect the flow in the axial direction. Moreover, for the same reason, the gap was sealed by two flexible annular rubber membranes expecially designed to have a negligible effect on the radial stiffness of the device. Anyway using a modular conception another version, involving two gap and one coil has been set up, using almost the same components (the entire set of components is shown in figure 7). The latter configuration is closer to that recently tested by other authors [16]. The comparative analysis of the two configurations could be the object of future investigation.
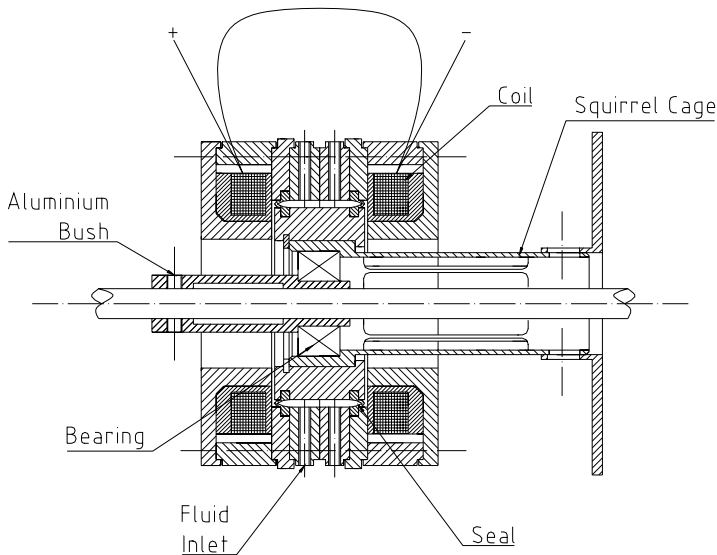
Fig.6   The MR fluid damper

Fig.7 Components realized

5.2 Design of the magnetic circuit

From the electromagnetic point of view the damper's structure can be considered as a circuit concentrating the magnetic field generated by the coils and guiding it through the MR fluid. An analysis of the magnetic behaviour of the device was carried out by using a finite elements code (ANSYS®) relating the value of the electric current running in the coils and the value of the magnetic field in the fluid. An axialsymmetric model was employed since the objective of the analysis was only to optimize the geometry of the magnetic circuit. Figures 8 and 9 show the values of the magnetic field and the flux lines in the device for a current density $J_S=7 \ A/mm^2$.
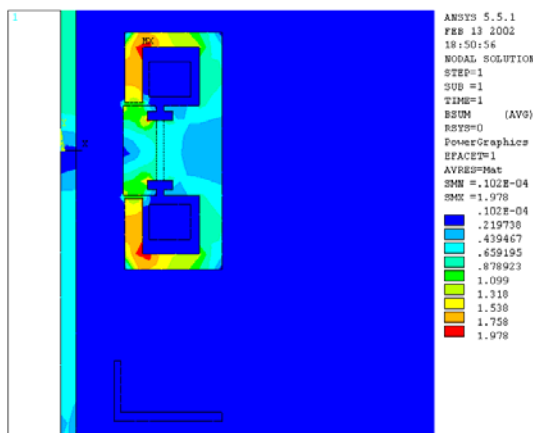
Fig.8 The magnetic field in the device
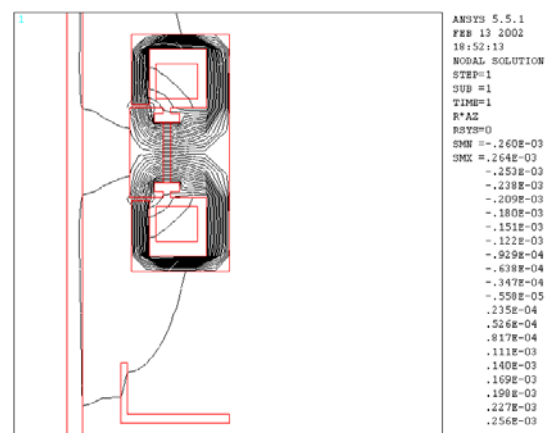
Fig 9 2-D Flux Lines

All materials magnetic properties are assumed linear, i.e, constant relative magnetic permeability (μ_r), μ_r=2000 for steel and μ_r=5 for the MR fluid. The linear relationship between the current density in the coils (measured in A/mm^2) and the magnetic field in the MR fluid B_{MR} (measured in *Tesla*) is expressed by the following equation:

$$B_{MR} = 7.15 \cdot 10^{-2} J_S \tag{8}$$

The bearing magnetic permeability was neglected because of the discontinuous structure (i.e.balls and plastic cage).

6. The test rig

The rotor, which was supplied with *Bently Nevada* *Rotor Kit*, is a slender *10 mm* diameter shaft, *560 mm* long. One or two discs of *0.8 kg* each can be fixed on the shaft. These discs have threaded holes at a radius of *30 mm* in order to create the desired unbalance inserting appropriate screw-weights. The shaft, supported by two adjustable oilite bearings, can reach a maximum rotational speed of *10.000 rpm*. The*Rotor- Kit* bench is equipped with eddy current probes for relative displacement measurements (3300 NSV™ Probe *Proximitor ®*).

The damper is supported by an alluminium ring connected to the pedestal of the *Rotor–Kit*, and is mounted on the shaft by means of the aluminium bush shown in fig. . It is connected to a current generator (*Hewlett – Packard E3611A DC power supply*) in order to feed the coil with a maximum constant current of *1.5A*.
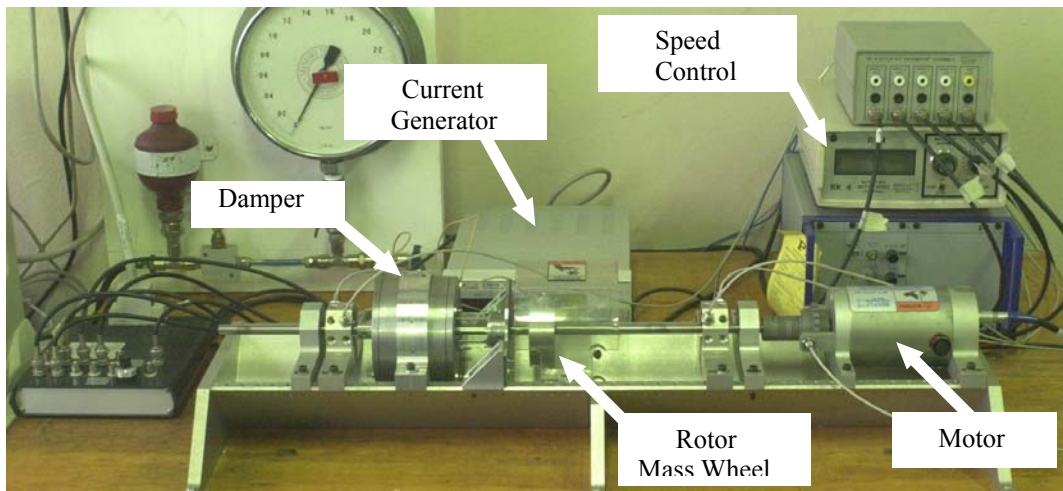
Fig.10 The test – rig

7. Preliminary tests

Preliminary tests have been performed. In the tested configuration the oilite bearings were *440 mm* apart and the damper was placed at a distance of *110 mm* from one of them. The disk was unbalanced with a *7g* grain. This value appears quite high in relation to the shaft and disk dimensions. Anyway during the numerical simulations it was observed that such an unbalance is necessary to test the characteristics of the MR fluid used since a lighter grain wouldn't be able to break the columnar structure created in the fluid and activate the damper unless the yield stress was extremely smaller.
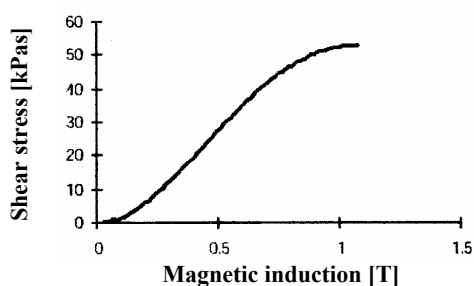
Fig.11 Shear stress vs magnetic induction in the fluid

The sensors were placed at a distance of *3 cm* from the oilite bearing farther from the damper. They were placed not too close to the whirling disk in order to avoid off – scale problems since the tests are characterized by great deformation of the shaft.

Rotational speed varying from *1000* up to *5000 rpm* were investigated at first, verifying the behaviour of the damper with no field applied and then feeding the coil with two different values of current: *0.5A* and *1A*. The calculated corresponding fields generated in the fluid, according to eq. (8), are *0.25T* and *0.12T* respectively.

The corresponding yield stress values of *8000Pa* and *3000Pa* are found from the relation shown in Fig.11. Figure 12 shows the value of the radial displacement of the shaft vs the rotational speed.
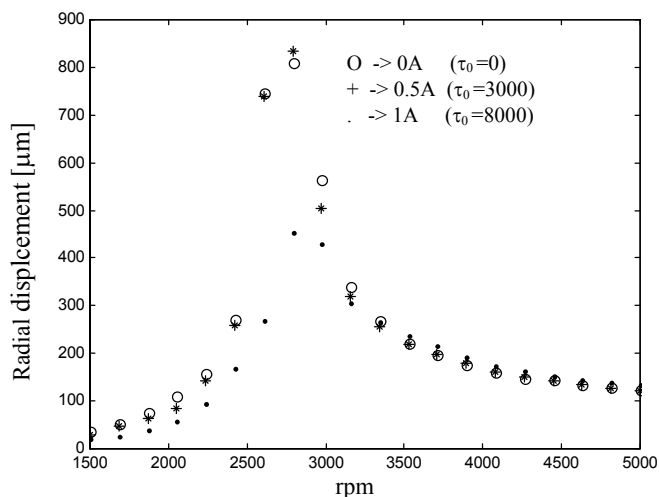
Fig.12 First experimental result

The magnetic field takes effect only when it becomes greater than *0.12T* and a significant reduction of the radial displacement of the shaft takes place for a yield stress equal to *8000Pa*. Compared to the numerical simulation the behaviour is similar to the expected one but there's a difference in the value of the effective yield stress. That can have different explanations. The first is related to the problem encountered in filling completely the gap. Then there might be some vacuum zones increasing the value of the current needed to generate the field and the corresponding yield stress. Such problems will be overcome in the next experimental campaign. Moreover, since during the motion the magnetic field in the device is not axialsymmetric, the magnetic field in the fluid and, consequently the yield stress, might vary significantly along the angular coordinate. Finally there might be some non linearities not taken into account in the analytical model.

8. Conclusions

In this paper a magnetorheological fluid squuze film damper has been presented. The simulation of the operation conditions have given indacation for the damper design. The preliminary experimental results obtained with the developed device shoew its effectivness in dampening the rotor vibrations controlling its dynamic characteristics by simply varying the current in the magnetic coils.An extensive experimental investigation is planned for the near future on the described device and on a modified configuration.

9. References

[1]   Bonneau O. and Frene J. (1997): Non-linear behavior of a flexible shaft partly supported by a squeeze film damper. - Wear, vol.206, pp.244-250.
[2]   Morishita S. and Tamaki U. (1993): ER fluid applications to vibration control devices and an adaptive neural-net controller. - J. Intelligent Material Systems and Structures, vol.4, pp.366-372.
[3]   Weiss PK., Carlson J.D., Duclos G.T., Chrzan M.J. and Margida A.J.: High strength magneto- and electro-rheological fluids. - SAE paper 932451,1993.
[4]   Shakeri C., Noori M.N. and Hou Z. (1996): Smart materials and structures, a review. - Proceedings of the 1996 4th Materials Engineering Conference, part 2, Washington DC, Materials for the New Millennium Proceedings of the Materials Engineering Conference, vol.2, ASCE, New York, pp.863-876.
[5]   Carlson J.D. and Weiss K.D. (1994): A growing attraction to magnetic fluids. - Machine Design, August 8, pp.61-64.
[6]   Tichy J.A. (1991): Hydrodynamic lubrication theory for the Bingham plastic flow model. - J. Rheology, vol.35, No.4, pp.477-496.
[7]   Tichy J.A. (1993): Behavior of a squeeze film damper with electrorheological fluid. - STLE Tribology Transactions, vol.36, No.1, pp.127-133.
[8]   Dimarogonas A.D. and Kollias A. (1992): Electorheological fluid-controlled "smart" journal bearings. - STLE Tribology Transactions, vol.35, No.4, pp.611-618.
[9]   Jung S.Y. and Choi S.B. (1995): Analysis of a short squeeze-film damper operating with electrorheological fluids. - STLE Tribology Transactions, vol.38, No.4, pp.857-862.
[10] Morishita S. and An Y.K. (1996): On dynamic characteristics of ER fluid squeeze film damper. - JSME International Journal, series C, vol.39, No.4, pp.702-707.
[11] Nikolakopoulos P.G. and Papadopoulos C.A. (1998): Controllable high speed journal bearings, lubricated with electro-rheological fluids. An analytical and experimental approach. - Tribology International, vol.31, No.5, pp.225-234.
[12] Kordonsky W.I. (1993): Magnetorheological effect as a base of new devices and technologies. - J. of Magnetism and Magnetic Materials, vol.122, pp.395-398.
[13] Jolly M.R. and Carlson J.D. (1996): Controllable squeeze film damping using magnetorheological fluid. - Proc. 5th International Conference on New Actuators, 26-28 June 1996, Bremen, Germany, pp.333-336.
[14] Jolly M.R., Bender J.W. and Carlson J.D. (1998): Properties and applications of commercial magnetorheological fluids. - Spie 5th Annual Int. Symposium on Smart Structures and Materials, San Diego, CA, 15 March 1998.
[15] Bolter R. and Janocha H.: Design rules for MR fluid actuators in different working modes. - SPIE, vol.3045, pp.148-159.
[16] Zhu C., Robb D.A., Ewins D.J. (2001): Magnetorheological fluid dampers for rotor vibration control. – AIAA 2001 – 1469, pp.2121-2127.